



Transport anomaly at the ordering transition for adatoms on graphene

Sergey Kopylov,¹ Vadim Cheianov,¹ Boris L. Altshuler,² and Vladimir I. Fal'ko¹¹*Department of Physics, Lancaster University, Lancaster, LA1 4YB, UK*²*Physics Department, Columbia University, New York, New York 10027, USA*

(Received 20 April 2011; published 17 May 2011)

We analyze a manifestation of the partial ordering transition of adatoms on graphene in resistivity measurements. We find that the Kekulé mosaic ordering of adatoms increases the sheet resistance of graphene due to a gap opening in its spectrum and that critical fluctuations of the order parameter lead to a nonmonotonic temperature dependence of resistivity with a cusp-like minimum at $T = T_c$.

DOI: [10.1103/PhysRevB.83.201401](https://doi.org/10.1103/PhysRevB.83.201401)

PACS number(s): 72.80.Vp, 05.70.Fh

Impurities in metals experience a long-range Ruderman-Kittel-Kasuya-Yosida (RKKY) interaction due to polarization of the electron Fermi sea (Friedel oscillations).¹ For surface adsorbents such an interaction may result in their structural ordering, repeating the pattern of the Friedel oscillations of electron density.² In particular, a dilute ensemble of adatoms on graphene may undergo a partial ordering transition.³⁻⁶

Unlike other materials, the RKKY interaction between adatoms on graphene exists even at zero carrier density, with a characteristic long-range $1/r^3$ dependence, and it exhibits Friedel oscillations which are commensurate with the underlying honeycomb lattice. For adatoms residing above the centers of the honeycombs, the intervalley scattering of the electrons by adatoms leads to Friedel oscillations that resemble a $\sqrt{3} \times \sqrt{3}$ charge-density wave superlattice. Positions of each individual adatom relative to such superlattice can be characterized by one of three vectors, $\mathbf{u} = (\cos \frac{2\pi m}{3}, \sin \frac{2\pi m}{3})$ with $m = -1, 0, 1$. The transition of an ensemble of adatoms into a “Kekulé mosaic” ordered state,³ characterized by the order parameter $\bar{\mathbf{u}}$, falls in the symmetry class of three-state Potts models.⁷

In this paper we analyze how partial “Kekulé” ordering of adatoms on graphene affects its resistivity ρ in the regime of low coverage, $n_i a^2 \ll 1$ (n_i is the concentration of adatoms, a is the lattice constant). The behavior of the temperature-dependent resistivity correction $\delta\rho(T) = \rho(T) - \rho(\infty)$ is sketched in Fig. 1. At $T \ll T_c$ (region I) the temperature dependence of the resistivity is dominated by a nonvanishing order parameter $\bar{\mathbf{u}}$ causing the amplified intervalley mixing and opening a gap $\Delta \propto \bar{\mathbf{u}} \sim (T_c - T)^\beta$ in the corners of the Brillouin zone. As the temperature increases from $T = 0$ to $T = T_c$ the resistivity correction monotonically decreases as $(T_c - T)^{2\beta}$. At $T > T_c$, critical fluctuations of the order parameter, which are characterized by the correlation length $\xi \propto |T - T_c|^{-\nu}$ and precede the formation of the ordered phase, lead to a nonmonotonic feature in $\delta\rho(T)$. At high temperature, $T \gtrsim T_c$ (region III), the constructive interference of electron waves, scattered by adatoms within ordered clusters of size ξ , enhances resistivity. The effect, which becomes stronger upon approaching T_c , is similar to the critical opalescence⁸ in materials undergoing a structural phase transition or the resistivity anomaly in bulk metals with magnetic impurities undergoing a ferromagnetic transition.⁹ This enhancement saturates when ξ becomes comparable to the electron wavelength λ_F (i.e., $\lambda_F \approx \xi$). In region II

of temperatures $T \rightarrow T_c + 0$, where $\xi \gg \lambda_F$, scattering of electrons is affected only by the gradient of the fluctuating order parameter $\bar{\mathbf{u}}$. The resistivity is thus reduced and a cusp-shape minimum at $T = T_c$ should be expected.

In the following we assume that the electron concentration $n_e = 4\pi/\lambda_F^2$ is not high (i.e., $n_e \ll n_i$), but the electron Fermi wavelength is shorter than its mean-free path, $\lambda_F \ll l$. This assumption also implies that, in the ordered phase, $k_B T, \Delta \ll \varepsilon_F$.

The electrons are described by a four-component Dirac-like spinor $\Psi = [\psi_{K,A}, \psi_{K,B}, \psi_{K',B}, \psi_{K',A}]$ with the components corresponding to different valleys (K, K') and sublattices (A, B).¹⁰ In the absence of adatoms, quasiparticles are characterized by the linear spectrum $|\varepsilon_{\mathbf{p}}| = \hbar v p$ and plane-wave states (for $\varepsilon_{\mathbf{p}} > 0$):

$$|K\mathbf{p}\rangle = \frac{e^{i\mathbf{p}\mathbf{r}}}{\sqrt{2S}} \begin{pmatrix} 1 \\ e^{i\varphi_{\mathbf{p}}} \\ 0 \\ 0 \end{pmatrix}, \quad |K'\mathbf{p}\rangle = \frac{e^{i\mathbf{p}\mathbf{r}}}{\sqrt{2S}} \begin{pmatrix} 0 \\ 0 \\ 1 \\ -e^{i\varphi_{\mathbf{p}}} \end{pmatrix}.$$

Here, S is the area of the graphene sheet and $\mathbf{p} = (p \cos \varphi_{\mathbf{p}}, p \sin \varphi_{\mathbf{p}})$ is the electron wave vector.

The Hamiltonian describing graphene covered by adatoms has the form^{3,11}

$$\hat{H} = \hbar v(\mathbf{p}\Sigma) + \hat{U}(\mathbf{r}) + \hat{V}(\mathbf{r}), \quad \hat{U} = \sum_l \hat{I} w(\mathbf{r} - \mathbf{r}_l), \quad (1)$$

$$\hat{V} = \hbar \lambda v a \sum_l \Sigma_z(\mathbf{u}_l \Lambda) \delta(\mathbf{r} - \mathbf{r}_l).$$

We assume that the dimensionless impurity potential λ is small ($\lambda \lesssim 1$) and will treat the electron-adatom interaction perturbatively. We use the set^{2,11} of 4×4 “sublattice” and “valley” matrices $\Sigma_x, \Sigma_y, \Sigma_z$ and $\Lambda_x, \Lambda_y, \Lambda_z$:

$$\Sigma_x = \Pi_z \otimes \sigma_x, \quad \Sigma_y = \Pi_z \otimes \sigma_y, \quad \Sigma_z = \Pi_0 \otimes \sigma_z,$$

$$\Lambda_x = \Pi_x \otimes \sigma_z, \quad \Lambda_y = \Pi_y \otimes \sigma_z, \quad \Lambda_z = \Pi_z \otimes \sigma_0,$$

where σ_i and Π_j are Pauli matrices in the sublattice (AB) and valley (KK') spaces.

The form of the electron-adatom interaction in Eq. (1) is prescribed by the highly symmetric position of adatoms at the centers of hexagons. The \hat{U} term does not violate the AB sublattice symmetry and scatters electrons without changing their valley state. The \hat{V} term²⁻⁴ is responsible for the intervalley scattering of electrons. The sensitivity of the

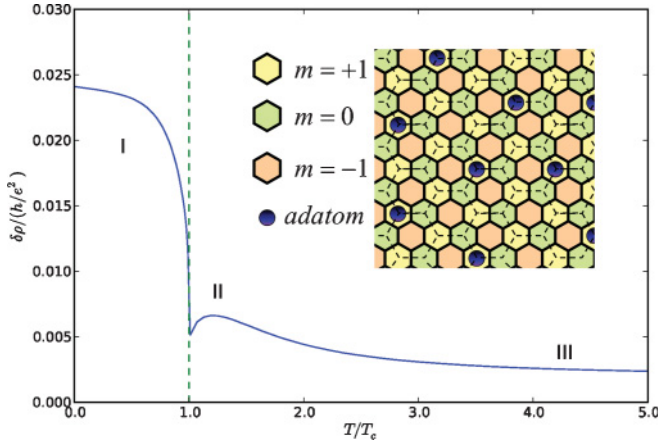


FIG. 1. (Color online) The predicted anomaly in the temperature-dependent resistivity of graphene decorated with adatoms in the vicinity of the Kekulé ordering transition. The inset illustrates the Kekulé mosaic ordered state and the assignment of Potts “spin” $m = -1, 0, 1$ to various hexagons in the $\sqrt{3} \times \sqrt{3}$ superlattice.

scattering phase of an electron to the position of the adatom in the $\sqrt{3} \times \sqrt{3}$ superlattice manifests itself by the Potts parameter \mathbf{u} in the intervalley term.

Each adatom creates Friedel oscillations of the electron density leading to the RKKY-type interaction between adatoms. The contribution of the \hat{U} term, Eq. (1), to such an interaction is a $1/r^3$ repulsion independent of the Potts spins. At the same time the symmetry-breaking coupling leads to the three-state Potts model with a long-range interaction $-\mathbf{u}_j \cdot \mathbf{u}_l/r_{jl}^3$.

To minimize the interaction energy, adatoms have to take equivalent positions within the $\sqrt{3} \times \sqrt{3}$ superlattice unit cells. A Monte Carlo simulation of the corresponding $1/r^3$ random-bond Potts model³ has revealed such an ordered phase below the transition temperature $T_c \approx 0.6\lambda^2(n_i a^2)^{3/2}\hbar v/a$.

The effects of adatoms ordering on the electron transport are encoded in the correlation function:

$$\overline{u^\alpha(\mathbf{r})u^\beta(\mathbf{r}') - u^\alpha(\mathbf{r})\overline{u^\beta(\mathbf{r}')}} = \delta_{\alpha\beta}g(|\mathbf{r} - \mathbf{r}'|),$$

for which the theory of critical phenomena predicts the scaling form¹²

$$g(r) = \frac{\kappa(r/\xi)}{(\sqrt{n_i}r)^\eta}, \quad \kappa(y) = \kappa_1(y) + y^{\frac{1-\alpha}{\nu}}\kappa_2(y). \quad (2)$$

Here, $\xi \sim n_i^{-1/2}|(T - T_c)/T_c|^{-\nu}$ is the correlation length, and α , η , and ν are critical exponents. It has been shown⁷ that, for the three-state Potts model on a square lattice, $\eta = 4/15$; however, the value of η for the random-bond Potts models with a long-range interaction is still unknown.^{13,15} In the critical region $r \ll \xi$, the correlation function has essentially an $r^{-\eta}$ behavior, with a correction (second term) related to the specific heat anomaly $C \sim |T - T_c|^{-\alpha}$.⁷ At large distances, $r \gg \xi$, $g(r)$ decays exponentially, according to the Ornstein-Zernike theory.^{12,16} Overall, for $T > T_c$ the scaling functions $\kappa_{1,2}(y)$ have the following asymptotics:

$$\begin{aligned} \kappa_1(y \ll 1) &\approx c_1, \quad \kappa_2(y \ll 1) \approx -c_2, \quad (c_1, c_2 \sim 1); \\ \kappa_1(y \gg 1) &\propto \frac{e^{-y}}{y^{1/2-\eta}}, \quad \kappa_2(y \gg 1) \sim e^{-y}, \end{aligned} \quad (3)$$

whereas for $T < T_c$,

$$\begin{aligned} \kappa_1(y \ll 1) &\approx c_1, \quad \kappa_2(y \ll 1) \approx c_2; \\ \kappa_1(y \gg 1) &\propto \frac{e^{-y}}{y^{2-\eta}}, \quad \kappa_2(y \gg 1) \sim e^{-y}. \end{aligned}$$

At $T < T_c$, the order parameter also acquires a homogeneous average $\bar{\mathbf{u}} \propto (T_c - T)^\beta$. As long as $\bar{\mathbf{u}}$ exceeds the fluctuations of \mathbf{u} (i.e., far enough from T_c), the electron states whose wavelength is larger than the distance $n_i^{-1/2}$ between adatoms are described by the effective mean-field Hamiltonian:

$$\bar{H} = \hbar v \mathbf{p} \Sigma + n_i \hbar \lambda v a \Sigma_z (\bar{\mathbf{u}} \Lambda).$$

Accordingly, the spectrum $\varepsilon_p^2 = (\hbar v p)^2 + \Delta^2$ acquires a gap:

$$\Delta(T) \approx n_i \hbar \lambda v a (1 - T/T_c)^\beta, \quad (4)$$

such that $\Delta(0) \gg T_c$. The plane-wave eigenstates of \bar{H} are mixed between the two valleys and take the form (for $\varepsilon_p > 0$)

$$|\pm 1, \mathbf{p}\rangle = \frac{e^{i\mathbf{p}\mathbf{r}}}{\sqrt{4S}} \begin{pmatrix} \sqrt{\frac{\varepsilon_p \pm \Delta}{\varepsilon_p}} \\ \sqrt{\frac{\varepsilon_p \mp \Delta}{\varepsilon_p}} e^{i\varphi_p} \\ \pm \sqrt{\frac{\varepsilon_p \pm \Delta}{\varepsilon_p}} e^{i\theta} \\ \mp \sqrt{\frac{\varepsilon_p \mp \Delta}{\varepsilon_p}} e^{i(\varphi_p + \theta)} \end{pmatrix}, \quad \bar{u}_x + i\bar{u}_y = u e^{i\theta}.$$

Intravalley and intervalley scattering determined by $\hat{U}(\mathbf{r})$ and $\hat{V}(\mathbf{r})$ in Eq. (1), respectively, do not interfere with each other. Hence, the total momentum relaxation rate is the sum of the two electron scattering rates:

$$\tau^{-1} = \tau_0^{-1} + \tau_i^{-1}, \quad (5)$$

where τ_0 and τ_i stand for intravalley and intervalley momentum relaxation times. For the temperature-dependent Drude resistivity of graphene sheets (recall that $k_B T, \Delta \ll \varepsilon_F$) we thus have

$$\rho(T) = \frac{2}{e^2} \frac{1}{v_F^2 \tau \nu}, \quad (6)$$

where $v_F = \hbar v^2 p_F / \varepsilon_F$ is the Fermi velocity, $\nu = 2\varepsilon_F / (\pi \hbar^2 v^2)$ is the density of states, and the Fermi energy and momentum are related to the electron density as $p_F = \sqrt{\pi n_e}$ and $\varepsilon_F = \sqrt{\pi \hbar^2 v^2 n_e + \Delta^2}$.

The temperature dependence of $\rho(T)$ at $T \lesssim T_c$ is dominated by the effect of the order parameter $\bar{\mathbf{u}}$ on the chiral plane-wave functions and thus on the scattering rates; in particular τ_0^{-1} . In the Born approximation,

$$\begin{aligned} \frac{1}{\tau_0} &= \frac{n_i p_F^2}{\hbar \varepsilon_F} \int_0^{2\pi} \frac{d\varphi}{2\pi} \tilde{w}^2 \left(2p_F \sin \frac{\varphi}{2} \right) (1 - \cos \varphi) r_0(\varphi), \\ r_0(\varphi) &= \cos^2 \frac{\varphi}{2} + \frac{\Delta^2(T)}{(\hbar v p_F)^2}, \end{aligned} \quad (7)$$

where $\tilde{w}(k) = \int d\mathbf{r} e^{i\mathbf{k}\mathbf{r}} w(r)$ and φ is the scattering angle. The form factor $r_0(\varphi)$ arises from the overlap integral between

plane-wave states and reflects the absence of the backscattering for $\Delta = 0$. Thus, for $T \lesssim T_c$, we find

$$\frac{\delta\rho(T)}{\rho(\infty)} \approx \frac{4\Delta^2(T)}{\pi n_e \hbar^2 v^2} \frac{\int_0^{2\pi} d\varphi \tilde{w}^2 (2p_F \sin \frac{\varphi}{2}) \sin^2 \frac{\varphi}{2}}{\int_0^{2\pi} d\varphi \tilde{w}^2 (2p_F \sin \frac{\varphi}{2}) \sin^2 \varphi}. \quad (8)$$

The temperature dependence of $\rho(T)$ at $T > T_c$ is determined by the effect of the ordering of adatoms on the intervalley scattering. Consider the scattering amplitude

$$\langle K' \mathbf{p}' | \hat{V} | K \mathbf{p} \rangle = \frac{\hbar \lambda v a}{2iS} \sin \left(\frac{\varphi_{\mathbf{p}} + \varphi_{\mathbf{p}'}}{2} \right) \sum_l e^{i\theta_l}, \quad (9)$$

$$\theta_l = \frac{2\pi m_l}{3} + (\mathbf{p} - \mathbf{p}') \mathbf{r}_l.$$

At temperatures far from T_c (i.e., $T \gg T_c$), adatom positions on the superlattice are random so that m_l take on the values of $-1, 0$, and 1 with equal probabilities. As a result, the absolute value of the scattering amplitude can be estimated as $|\langle K' \mathbf{p}' | \hat{V} | K \mathbf{p} \rangle| \sim (n_i \lambda_F^2)^{1/2}$. Upon approaching T_c from above, clusters of ordered adatoms with a characteristic size $\xi \gg n_i^{-1/2}$ start appearing. In the sum (9), such a cluster generates constructive interference between terms with the same value of m_l provided that $\xi \lesssim \lambda_F$. This increases the scattering amplitude, $|\langle K' \mathbf{p}' | \hat{V} | K \mathbf{p} \rangle| \sim n_i \xi \lambda_F$. A further increase in the correlation length, $\xi > \lambda_F$, has the opposite effect on scattering: electrons get scattered only by gradients in the smoothly fluctuating field $\bar{\mathbf{u}}$.

The intervalley momentum relaxation rate (both at $T < T_c$ and $T > T_c$)¹⁷ τ_i^{-1} can be expressed in terms of the Fourier transform of the correlation function, $\tilde{g}(k) = \int d\mathbf{r} e^{i\mathbf{k}\mathbf{r}} g(r)$,

$$\frac{1}{\tau_i} = \frac{\hbar v^2 p_F^2 n_i \lambda^2 a^2}{2\varepsilon_F} \int_0^{2\pi} \frac{d\varphi}{2\pi} (1 - \cos \varphi) r_i(\varphi),$$

$$r_i(\varphi) = \left[1 + n_i \tilde{g} \left(2p_F \sin \frac{\varphi}{2} \right) \right] \left[2 \sin^2 \frac{\varphi}{2} + \frac{\Delta^2(T)}{(\hbar v p_F)^2} \right]. \quad (10)$$

At $T > T_c$ ($\Delta = 0$), the temperature dependence of $\rho(T)$ comes from the correlation function $\tilde{g}(k)$ in Eq. (10). Far from the phase transition, $|T - T_c| \sim T_c$, where $\xi < \lambda_F$ (region III in Fig. 1), electrons are effectively scattered by small clusters of ordered adatoms. In this region we approximate $\tilde{g}(k) \approx \tilde{g}(0) \propto (\sqrt{n_i} \xi)^{2-\eta}$ and find that

$$\delta\rho(T) \approx C \frac{\Delta^2(0)}{e^2 v^2 \hbar n_i^{\eta/2}} \xi^{2-\eta} \propto \frac{n_i^{2-\eta/2}}{(T - T_c)^{(2-\eta)v}}, \quad (11)$$

where $C = (3\pi^2/2) \int_0^{+\infty} dy y^{1-\eta} \kappa(y)$ is a dimensionless constant.

In the vicinity of the critical point, such that $\lambda_F < \xi$ (region II in Fig. 1), electrons experience multiple scatterings within one cluster with a small wave-vector transfer, $\sim \xi^{-1}$. This makes $\rho(T)$ sensitive to the critical behavior of the correlation function at $r < \xi$. This region is easier to analyze by performing the angular integration in Eq. (10) and expressing τ_i^{-1} in terms of the function $\kappa(y)$ defined in Eq. (2):

$$\frac{1}{\tau_i} = \frac{\Delta^2(0)}{\hbar^2 v} \left[\frac{3p_F}{4n_i} + \frac{2\xi}{(\sqrt{n_i} \xi)^\eta} \int_0^{+\infty} dy \frac{\kappa(y)}{y^\eta} f(p_F \xi y) \right]. \quad (12)$$

Here, f can be expressed in terms of Bessel functions as

$$f(x) = \frac{\pi}{x} [x^2 J_0^2(x) - x^2 J_1^2(x) + J_1^2(x) - x J_0(x) J_1(x)].$$

To evaluate the integral in Eq. (12) we divide the integration interval $[0, \infty]$ into two parts, $[0, y_0]$ and $[y_0, \infty]$, where $1 \gg y_0 \gg 1/(p_F \xi) \rightarrow 0$. For the interval $[y_0, \infty]$, we use the fact that $f(p_F \xi y)$ is a fast oscillating function, $f(x \gg 1) \approx 2 \sin(2x) + 3 \cos(2x)/(2x)$, and that

$$\int_{y_0}^{+\infty} F(y) \sin(Ay) dy = \frac{F(y_0) \cos(Ay_0)}{A} + O\left(\frac{1}{A^2}\right),$$

for $A \gg 1$ and $F(\infty) = 0$. For the interval $[0, y_0]$ and to leading order in $1/p_F \xi$, the result is determined by the values of $\kappa_1(0)$ and $\kappa_2(0)$ in Eq. (3). For this, we expand κ_1 and κ_2 (which vary at the scale of $y \sim 1$) into Taylor series, evaluate the corresponding integrals to leading orders in $y_0 \ll 1$, and combine the result with the contribution from the interval $[y_0, \infty]$. As a result, the term with κ_1 in Eq. (12) produces a finite contribution when $p_F \xi \rightarrow \infty$, and we find that

$$\rho(T_c) - \rho(\infty) = \frac{c_1 \pi^{3/2} \Delta^2(0)}{e^2 v^2 \hbar n_i} B(\eta) \left(\frac{n_i}{\pi n_e} \right)^{1-\eta/2}, \quad (13)$$

where $B(x) = x \Gamma(\frac{3+x}{2}) \Gamma(1 - \frac{x}{2}) / [\Gamma(1 + \frac{x}{2}) \Gamma(2 + \frac{x}{2})]$. If $(1 - \alpha)/\nu < 1$, the next term in the expansion $\kappa_1(y) = \kappa_1(0) + y \kappa_1'(0) + \dots$ generates a contribution $O[1/(p_F \xi)]$, which, for $T \rightarrow T_c$, is less relevant than the more singular $(T - T_c)$ -dependent¹³ contribution from the κ_2 term in Eq. (12). Following the same steps, we find that the latter term gives rise to the cusp in the $\rho(T)$ dependence in region II near T_c in Fig. 1:

$$\frac{\rho(T) - \rho(T_c)}{\rho(T_c) - \rho(\infty)} = -\frac{c_2 B(\eta - 2\gamma)}{c_1 B(\eta) (\pi n_e \xi^2)^\gamma} \propto (T - T_c)^{1-\alpha}, \quad (14)$$

where $\gamma = (1 - \alpha)/2\nu$, which is assumed to be $\gamma < 1/2$ for Eq. (14) to be applicable. Otherwise (for $\gamma > 1/2$) one should use

$$\frac{\rho(T) - \rho(T_c)}{\rho(T_c) - \rho(\infty)} = -\frac{\kappa_1'(0) B(\eta - 1)}{c_1 B(\eta) (\pi n_e \xi^2)^{1/2}} \propto (T - T_c)^\nu. \quad (15)$$

The sign of the result of Eqs. (14) and (15) is determined by the sign of c_2 [or $\kappa_1'(0) < 0$] and values of the critical exponents, where c_2 depends on the particular form of the correlation function $g(r)$ and is known to be positive for the exact solution of the two-dimensional (2D) Ising model on a square lattice.¹² The factor $B(\eta - 2\gamma)/B(\eta)$ has the same sign as $(\eta - 2\gamma)$ and happens to be negative for the three-state Potts model on a square lattice. Notice that Eqs. (14) and (15) are applicable only in the very close vicinity of T_c ($\xi \gg \lambda_F$) and do not influence the overall tendency of resistance to dip in region II.

The behavior of $\delta\rho(T)$ at $T < T_c$ (region I in Fig. 1) is determined by two contributions. One part, $\delta\rho_1/\rho \propto (T_c - T)^{\min\{1-\alpha, \nu\}}$, is related to the specific-heat-anomaly correction to the correlation function and can be obtained the same way as Eq. (14). The other contribution, $\delta\rho_2/\rho \propto (T_c - T)^{2\beta}$, is due to the formation of a nonzero order parameter in the Kekulé-ordered phase. The second correction dominates when $2\beta < \min\{1 - \alpha, \nu\}$, which is the case for the expected values of critical exponents.¹³ As a result, we attribute the rise of resistivity at $T < T_c$ near the cusp at $T = T_c$ to the formation

of a spectral gap in graphene due to the Kekulé mosaic ordering. The qualitative behavior of the resistivity correction as a function of temperature for all three regimes is plotted in Fig. 1 for $\varepsilon_F = 0.4v\sqrt{n_i}$ and $n_i\lambda^2a^2 = 0.005$,¹³ where we used the values $c_1 = 0.5$ and $c_2 = 0.15$ (calculating the exact values of these coefficients is outside the scope of this paper).

In conclusion, we investigated electron transport in graphene covered by a dilute ensemble of adatoms residing over the centers of hexagons. We calculated the temperature dependence of the resistivity $\rho(T)$, which appears to be nonmonotonic and has a nonanalytic cusp at $T = T_c$. Since the form of the cusp depends on the critical indices α and β

of the phase transition, experimental observation of such an anomaly may facilitate their measurements. The form of $\rho(T)$ shown in Fig. 1 appears to be generic for partially ordered dilute ensembles of adatoms with alternative positioning on the honeycomb lattice, such as over carbon-carbon bonds,⁴ since this also falls in the class of three-value Potts models.

This work was supported by EPSRC under Grants No. EP/G041954 and No. EU-FP7 ICT STREP Concept Graphene, US DOE Contract No. DE-AC02-06CH11357, and The Royal Society.

¹J. Friedel, *Philos. Mag.* **43**, 153 (1952).

²V. V. Cheianov and V. I. Fal'ko, *Phys. Rev. Lett.* **97**, 226801 (2006); C. Bena, *ibid.* **100**, 076601 (2008); A. Bacsı and A. Virosztek, *Phys. Rev. B* **82**, 193405 (2010); N. M. R. Peres, L. Yang, and S.-W. Tsai, *New J. Phys.* **11**, 095007 (2009).

³V. V. Cheianov, V. I. Fal'ko, O. Syljuasen, and B. L. Altshuler, *Solid State Commun.* **149**, 1499 (2009).

⁴V. V. Cheianov, O. Syljuasen, B. L. Altshuler, and V. Fal'ko, *Phys. Rev. B* **80**, 233409 (2009).

⁵V. V. Cheianov, O. Syljuasen, B. L. Altshuler, and V. I. Fal'ko, *Europhys. Lett.* **89**, 56003 (2010).

⁶D. A. Abanin, A. V. Shytov, and L. S. Levitov, *Phys. Rev. Lett.* **105**, 086802 (2010).

⁷R. J. Baxter, *Exactly Solved Models in Statistical Mechanics* (Academic Press, 1982).

⁸V. L. Ginzburg and A. P. Levanyuk, *J. Phys. Chem. Solids* **6**, 51 (1958); *Sov. Phys. JETP* **12**, 138 (1961).

⁹M. E. Fisher and J. S. Langer, *Phys. Rev. Lett.* **20**, 665 (1968).

¹⁰J. W. McClure, *Phys. Rev.* **104**, 666 (1956).

¹¹E. McCann, K. Kechedzhi, V. I. Fal'ko, H. Suzuura, T. Ando, and B. L. Altshuler, *Phys. Rev. Lett.* **97**, 146805 (2006); K. Kechedzhi, E. McCann, V. I. Fal'ko, H. Suzuura, T. Ando, and B. L. Altshuler, *Eur. Phys. J. Special Topics* **148**, 39 (2007).

¹²M. E. Fisher, *Rep. Prog. Phys.* **30**, 615 (1967).

¹³Critical exponents, satisfying the relations $2\nu = 2 - \alpha$ and $2\beta = \nu\eta$, are unknown for the disordered Potts model. Thus, we use the exponents of the three-state Potts model on a square lattice as a reference: $\alpha = 1/3$, $\beta = 1/9$, $\nu = 5/6$, and $\eta = 4/15$ ⁷. The small universal corrections to these values due to weak disorder were derived by Dotsenko.¹⁵ Note that the three-state Potts model with a $1/r^3$ interaction in 2D without disorder features a first-order phase transition; however, disorder makes it the second-order transition.¹⁴

¹⁴M. Aizenman and J. Wehr, *Phys. Rev. Lett.* **62**, 2503 (1989).

¹⁵V. I. Dotsenko, M. Picco, and P. Pujol, *Nucl. Phys. B* **455**, 701 (1995).

¹⁶L. D. Landau and E. M. Lifshitz, *Statistical Physics I* (Butterworth-Heinemann, 1980).

¹⁷The Born approximation is applicable for this problem only if the electron energy is larger than the average spectrum gap at the length scale of λ_F , $\Delta(\lambda_F) < \hbar v p_F$, where

$$\Delta(L) = \hbar n_i \lambda v a \sqrt{\mathbf{u}(\mathbf{r})\mathbf{u}(\mathbf{r}')_L} \sim \frac{\hbar \sqrt{n_i} \lambda v a}{L} (\sqrt{n_i} \min\{\xi, L\})^{1-\eta},$$

so that $\min\{\xi, \lambda_F\} < \frac{1}{\sqrt{n_i}} (\frac{4\pi^2}{n_i \lambda^2 a^2})^{1/(2-\eta)}$, which coincides with the inequality $v p_F \tau_i \gg 1$; that is, if the graphene resistivity is smaller than h/e^2 .